Experimental Observation on MS Plate Cooling by Air Jet in a Laboratory Scale ROT

Thesis submitted in partial fulfilment of

the requirements for the degree of

Master of Mechanical Engineering

By

Souvik Mukhopadhyay

Examination Roll No.: M4MEC1601

Registration No.: 111926 of 2010 - 2011

Under the guidance of

Sri Pranibesh Mandal

and

Prof. Swarnendu Sen

DEPARTMENT OF MECHANICAL ENGINEERING

FACULTY OF ENGINEERING & TECHNOLOGY

JADAVPUR UNIVERSITY

KOLKATA – 700032

MAY 2016

FACULTY OF ENGINEERING AND TECHNOLOGY

JADAVPUR UNIVERSITY

CERTIFICATE OF APPROVAL*

This foregoing thesis is hereby approved as a credible study of an engineering subject carried out and presented in a manner satisfactory to warrant its acceptance as a prerequisite to the degree for which it has been submitted. It is understood that by this approval the undersigned do not endorse or approve any statement made, opinion expressed or conclusion drawn therein but approve the thesis only for the purpose for which it has been submitted.

Committee _____

On Final Examination for

Evaluation of the Thesis _____

*Only in case the thesis is approved.

FACULTY OF ENGINEERING AND TECHNOLOGY

JADAVPUR UNIVERSITY

We hereby recommend that the thesis presented under our supervision by *Mr. Souvik Mukhopadhyay* entitled *"Experimental observation on MS plate cooling by air jet in a laboratory scale ROT"* be accepted in partial fulfillment of the requirements for the degree of Master of Mechanical Engineering.

Countersigned

Thesis Advisors

Head of the Department
Mechanical Engineering
Jadavpur University

Dean of Faculty of
Engineering and Technology
Jadavpur University

ACKNOWLEDGEMENT

I would like to express my sincere gratitude to my supervisor Sri Pranibesh Mandal and Prof. Swarnendu Sen for their valuable guidance, advice and encouragement throughout the course of this study and the writing of this thesis. Words of thanks will fall short to express my gratitude to them in proper dimensions for their kind co-operation and methodical guiding in course of the thesis work.

It is great pleasure for me to acknowledge my ineptness to Prof. Achintya Mukhopadhyay, Dr. Rana Saha and Head of the Mechanical Engineering Department Prof. Dipankar Sanyal for their time to time advice and assistance during this work. This has been a precious opportunity for me not only to gain knowledge and skill in the areas of fluid mechanics and heat transfer, but also to learn much more about approaches, attitudes towards work and interpersonal relationship.

I would like to express my deepest sense of gratitude to Shouvik Chowdhury, a research scholar of this department, for helping me out in every possible way throughout the course of my work. This thesis work would not have completed without his much valuable support.

I would also like to extend my heartfelt thanks towards the all the faculty members, research scholars and students associated with Project Neptune Laboratory, especially Niteshda, Shibuda, Prabir, Saptarshida, Dipakda, Uddalok, Krishnendu, Abu as their helping attitude without hesitation and encouragement during the whole process of the thesis work was really needed. I owe these people a lot for the wonderful times we spent together in our beloved lab.

I am indebted to undergraduate students Sudipta, Anurag, Sohag, Anuvab and Akibul greatly for their precious helping hands during the experiments. It would have been very difficult task to handle such a huge setup single-handedly without them.

In this respect, I would also like to grab this opportunity to express my heart-felt gratitude to my parents and sister without whose suggestions and hospitality it could have been difficult to carry out the project work and complete the thesis in time.

Last but not the least, constant support and motivation extended by my friend Anamitraa Chakraborty is deeply and appreciatively acknowledged.

Date: (Souvik Mukhopadhyay)

ABSTRACT

Ultra-Fast Cooling (UFC) technique due to its wide range of cooling rates has enabled the steel industries to obtain a large variety of new steel grades. The laminar cooling method used in traditional hot rolling mills has been replaced by UFC to a huge extent and also the size of run-out table (ROT) has been reduced from 85-90 m to ~ 5m. A laboratory scale model of a reciprocating ROT of less than 1.5m length and provisions for air or water or air-water mist spray cooling has been fabricated to study the cooling characteristics of steel plates. Experimental study of cooling characteristics of MS plates with different plate thickness have been carried out in stationary condition of the ROT using air jets from the nozzles on the both sides of the plate. Thermocouples have been attached in four different positions on the surface of the plate to measure the instantaneous temperature of the same in real-time during cooling. The temperature data, recorded by an NI-cRIO real-time system (RTS) have been analysed to study the effect of parameters like air flow rate (Q), initial temperature of the plate (T_{in}) and nozzle bank distance (D) on the cooling behaviour characterized by the average temperature of the plate (T_{avg}), cooling rate (θ) and convective heat transfer coefficient (h). Also an attempt to predict the empirical relationship among each of the involved parameters and T_{avg} has been made with the help of best fitted surface plots in Matlab, providing high accuracy of fitting according to the statistical measures.

CONTENTS

LIST OF FIGURES

LIST OF TABLES

NOMENCLATURE

A	Total area of the two surfaces under air jet (m^2)
c_p	Specific heat of Mild Steel (J/kg-^oC)
D	Nozzle bank distance (mm)
h	Heat transfer coefficient (W/m^2- ^oC)
m	mass of the plate (kg)
Q	Spray impingement flow rate (m^3/h)
t	Time (sec)
T	Instantaneous temperature (^oC)
T_∞	Ambient Temperature (^oC)
T_{avg}	Average temperature of the plate (^oC)
T_{in}	Initial temperature of the plate (^oC)
v	Velocity of the plate (m/sec)
θ	Cooling rate (^oC/sec)
ρ	Density of the Mild Steel (kg/m^3)

Chapter 1

Introduction and Literature Review

Hot rolling in steel industries involves strip cooling of the products at a controlled rate of 5~10 K/s to impart desirable metallurgical structures using a run out table (ROT). At these low cooling rate regimes, it is difficult to obtain advanced steel grades such as Dual Phase (DP), Transformation Induced Precipitation (TRIP) and multiphase (MP). In order to develop such new steel grades, Ultra Fast Cooling (UFC) under spray impingement with much faster and precisely controlled cooling rate has been introduced.

Water jets and sprays offering high rate of cooling in rolling mills, have been a regular topic of engineering research for a long time. The heat transfer coefficient reduced drastically above the Leidenfrost temperature for the case of spray quenching of steel billets heated above 1000°C, as investigated by Stewart et al. [1]. They measured the temperature using thermocouples. Li and Zhang [2] carried out finite element analysis of quenching with controlled cooling of moderately thick steel plates. Considering convection to be the mode of heat transfer they found out how factors like Jet Velocity, Initial Temperature of the steel plate, Temperature of the Cooling Water and plate Operating Speed influence the cooling process. Liu et al. [3] and Hauksson et al. [4] identified the various zones of impingement heat transfer and also the parameters that have significant effects over boiling heat transfer on stationary plates under water jet. Sozbir et al. [5] conducted experiments to investigate the heat transfer mechanism water mist impingement on high-temperature steel surface. They measured local heat transfer coefficient at various air velocities and liquid mass fluxes in the film boiling regime. They applied air velocity from 0 to 50.3m/s, liquid mass flux from 0 to 7.67kg/m^{2}s, and kept surface temperature of stainless steel between 525°C and 500°C. They found that the Leidenfrost temperature increases with both the air velocity and the liquid mass flux. Oisin et al. [6] developed a fully functional test rig to study the heat transfer characteristics of mist jets. After calibration they carried out experiments on that to conclude that heat transfer coefficient increases drastically with the introduction of a fine water mist, even at sub-boiling temperatures. They isolated heat transfer due to mist and estimated that as the total heat transfer minus the heat transfer due to air flow and wall interaction, and that owing to the cooling of the air by the droplets.

Horsky et al. [7] investigated effect of plate motion for spray cooling of long products with initial temperatures of about 350°C using reciprocating motion of the plate. Also, they observed that for wetted plate, increasing the plate speed caused reduction in the cooling rate when temperature reached 100°C. Yuan et al. [8] used finite difference method to evaluate the range of overall convective heat transfer coefficient to be approximately 4-8kW/m^{2}K when the cooling rate is 300-400^{o}C/s during ultra fast cooling of a 3-4mm thick steel strip. Wang et al. [9] carried out experiments under transient conditions, to reveal heat transfer phenomena of a hot static steel plate under multiple circular jets on top on an ROT. Local surface convective heat

transfer coefficients and corresponding temperatures have been calculated by a two-dimensional finite difference program based on inverse heat conduction model. They used cooling water jet flow rate from 15L/min to 35L/min and found that heat transfer coefficients are nonlinear functions of surface temperature and at stagnation point heat transfer coefficient and surface temperature are independent of the flow rate. Their analysis also yielded that heat transfer coefficient ratio changes slightly from 0.87 to 0.97, within 70mm distance from stagnation line whereas heat transfer coefficient ratio decreases with increasing distance from stagnation line beyond 350°C surface temperature. Hosain et al. [10] investigated the heat transfer of water jets impinging on a hot flat steel plate under temperatures below the boiling point to focus on the convection heat transfer phenomena which is a major step preceding the boiling. They simulated single axisymmetric jet and a pair of interacting jets using the RANS model under steady and transient conditions as well as the k-ε turbulence model considering both 2D axisymmetric and 3D simulations applying two sets of boundary conditions, constant temperature and constant heat flux at the surface of the steel plate.

Wang et al. [11] studied the effect of water flow rate on the heat transfer coefficient and surface temperature with the cooling water jet flow rate varied from 0.9 to 2.1m^3/h. Lee et al. [12] studied the effect of nozzle height on heat transfer of a hot steel plate cooled by an impinging liquid jet.

Wang et al. [13] investigated the effect of the initial surface temperature, water temperature and jet velocity on the heat transfer characteristics for the industrial applications. Their results revealed that the rewetting front propagation was considerably affected by the growth and detachment of the bubbles in the rewetting front region and the wetting velocity varied with the distance from the stagnant point. They took into account the effect of initial surface temperature, water temperature, and jet velocity to establish a regression equation to predict the value of maximum heat flux. Their work attempted to predict and to optimize the industrial applications of ultra-fast cooling technology.

An off-line model for heat transfer processes in a ROT have been developed by Mukhopadhyay and Sikdar [14] and later converted to an on-line model for predicting finishing temperature in the HSM at Tata Steel. Barman et al. [15] have done a detailed study on the thermal behavior during cooling of a steel strip that is cooled by multiple jets of pressurized water from both sides. They considered a system of 10 equally spaced water jets for each of the two strip surfaces and assumed the initial strip temperature and the water jet temperature to be 775^{o}C and 35^{o}C respectively with a strip height of 20mm. They considered an effective heat transfer coefficient to represent the jet and the surface interaction and discretized the governing equation on the basis of finite-volume method using a power-law scheme and solved that with the help of TDMA algorithm. They predicted the distribution of temperature within the strip and investigated the effect of strip velocity on the temperature distribution and corresponding cooling rate. Samanta

et al. [16] presented the visualization of heat-lines and isotherms during cooling process of a hot moving steel plate. They considered single water jet cooling and have taken initial temperature of the plate as 780^{o}C, water jet velocity as 0.8m/s, plate velocity as 0.1m/s, plate length as 1.5m, temperature of water jet as 38^{o}C and half plate thickness 12mm. They identified a thermally unaffected zone in the computational domain using a divider heat-line. Subsequently, the effects of water jet velocity (0.8-1.6m/s), plate velocity (0.1-0.6m/s) and heat transfer coefficient on the thermally unaffected zone and the heat transfer were predicted in their work.

Mandal [17] designed an experimental setup of a UFC using an ROT of very short length of less than 1.5m that uses reciprocating motion with negligible terminal accelerations to simulate constant velocity of traditional ROTs. There has been provision of use of water and air jet combinations for cooling. The same setup has been used in the present study. The idea is to experimentally determine the cooling characteristics of a small test plate heated in a furnace. The cooling characteristics depend on many factors like the spray impingement flow rate (Q), the distance of spray nozzles from the plate (D), the initial temperature of the heated plate (T_{in}), the velocity of the plate (v) and the thickness of the same. The idea is to determine the most efficient combination of the factors determining the cooling rate enabling the industries to use only the optimum amount of water under the spray cooling. It not only helps the overall process to become more efficient but also to optimize the amount of water being used for the purpose thereby saving the natural resource. However, in the present scenario primarily only air jet has been used to determine the experimental cooling characteristics. So here, instead of water, improvement of cooling rate will help to reduce the requisite amount of air. In a similar fashion, effect of water jet can also be determined, so also that of some combination of air-water mixture. However, these experimental ideas have been kept as future scopes. As far as the present experimental procedure is concerned, Mild Steel Plates of two different thicknesses have been heated in furnace and cooled to room temperature under different combinations of Q, T_{in} and D while the plate remains static i.e. v is equal to zero. From the experimental observations, the temporal change in average temperature (T_{avg}), cooling rate (θ) and heat transfer co-efficient (h) with the change in Q, T_{in} and D have been plotted separately and empirical relationships have been found by best fit curve in MATLAB. The effect of the plate velocity v however has also been kept as a future scope of work.

Chapter 2

System Description

The laboratory setup consists of a furnace, two nozzle banks, air supply line and water supply line to the nozzles, an electro-hydraulic actuation system (EHAS) to give the reciprocating motion to the specimen plate, fixtures to hold the specimen on the cooling bay consisting of roller fitted rails and mechanical handling zone in between the cooling bay and the furnace.

The furnace is chamber type and has 18 nos. of Kanthal GLOBAR SD Silicon Carbide heating elements lining on the two inner side walls of the chamber as shown in Fig.2.1. Maximum heating rate of the furnace is 15^{o}C/min. The control panel of the furnace is installed separately. There are voltage and current indicators on the control panel. There is a safety controller to limit the maximum achievable temperature. It can be set on different temperature values given in ^{o}C on the dial and the heaters will not go beyond that temperature on which it is set. The operator can control the heating process with the help of an Automatic PID type programmable temperature indicating controller. As shown in Fig.2.1 the furnace door operation is vertical lifting type and manual. A limit switch is provided to ensure switching off the heaters once the door is opened. Detailed specifications of the furnace are given in Table.2.1.

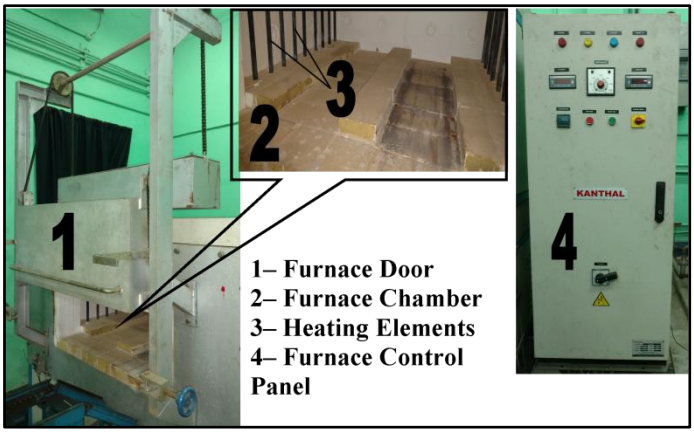

Fig.2.1: Furnace and Furnace Control Panel

Table.2.1: Furnace specifications

Description	Specification
Make	Kanthal, Sandvik Asia Ltd.
Serial number	SF-074
Working Chamber Dimensions	Depth: 800mm, Width: 800mm, Height: 300mm
Maximum Furnace Temperature	1200^{o}C
Power Rating	21kW
Power Supply	415 ± 10%V, 50 ± 5%Hz, 3-phase AC supply
Temperature Controller	Make: Eurotherm, Model: 2416

Two nozzle banks, each consisting of twenty nozzle units, are on the both sides of the cooling bay so that both the upward and downward surfaces of the specimen plate can be sprayed upon at the same time. There are two types of nozzles- long, round cross-section nozzles which spray water are called full cone hydraulic nozzles and rectangular cross-section nozzles which spray air-water mixture are called air mist nozzles. From Fig.2.2 it can be seen that there are 2 rows of hydraulic nozzles, 5 in each row on both sides of the plate which makes it a total of 20 of them. Similarly, there are 2 rows of air mist nozzles, 5 in each row on both sides of the plate which makes it a total of 20 of them too. Air mist and hydraulic nozzles are arranged in alternative rows. For any of the air atomizing or hydraulic nozzles, four nozzles on the four end positions of the two rows are connected to a common header and the rest of the six nozzles are connected to another header for each nozzle bank. As shown in Fig.2.2 headers of the air atomizing nozzles have square cross section and headers of the hydraulic nozzles have circular cross section. Water is supplied to the headers on both the sides of the cooling bay from a common pump. Pressurized air from a compressor comes to the square header leading to the mist spraying nozzles. Supplied air and water, as at high pressure, get thoroughly mixed in the square header and comes out as mist through the nozzles. If the water supply line to the mist spraying nozzles is closed then those nozzles can function as air spraying nozzles and cooling can be achieved using air only which exactly is done in this work. For the present work though only air cooling has been used. Heights of the nozzle banks can be adjusted using simple screw and nut mechanism. So the distance of the nozzle banks from the specimen plate can be varied to have different cooling rates. There is a clearance of 45mm between the nozzle bank and the specimen plate on any side when the nozzle bank is set at the zero mark on the scale attached with the setup. On that scale the distances of the nozzle banks can be varied from 0-140mm. Table.2.2 gives the specifications involved.

Air is first pressurized in a centrifugal compressor driven by a 3-phase induction motor and then supplied to the nozzle banks through a simple circuit that is connected to the upstream compressor line through a ball valve (BV). The circuit contains an air filter with manually operated regulator, a vortex flow meter (FM) and a pressure gauge associated with a needle valve to control the pressure setting. There is a 1" globe valve (GV) to control the flow of air in the line as shown in Fig.2.3. There is a pilot operated diaphragm type solenoid valve (SV), which is normally closed to regulate the flow of air. Before entering the headers of the mist spraying nozzles, the air supply line gets divided into two branches. One branch delivers air to the headers connecting 8 nozzles, and the other branch to the headers connecting 12 nozzles. Each branch is provided with separate ¾"GVs. Table.2.3 presents the component specifications.

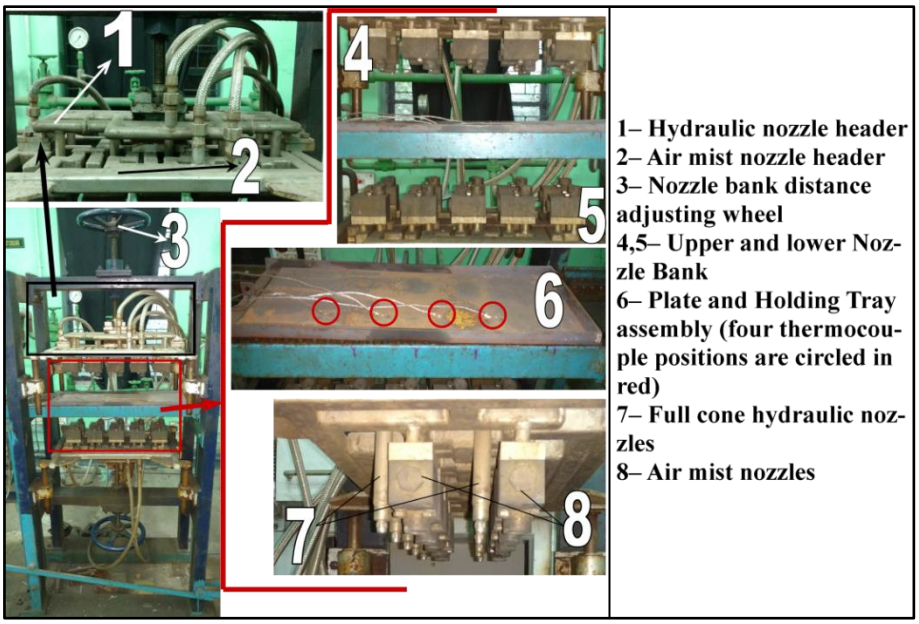

Fig.2.2: Nozzle Bank and Cooling Bay

Table.2.2: Nozzle Bank specifications

Component	Specification		
	Make	Nozzle No.	Maximum Flow rate per nozzle (Lpm)
Full Cone Hydraulic Nozzle	Lechler (India) Pvt. Ltd.	460.366.CA	0.7
Air Mist Nozzle	Lechler (India) Pvt. Ltd.	1PM.021.30.40.00.1	5.8

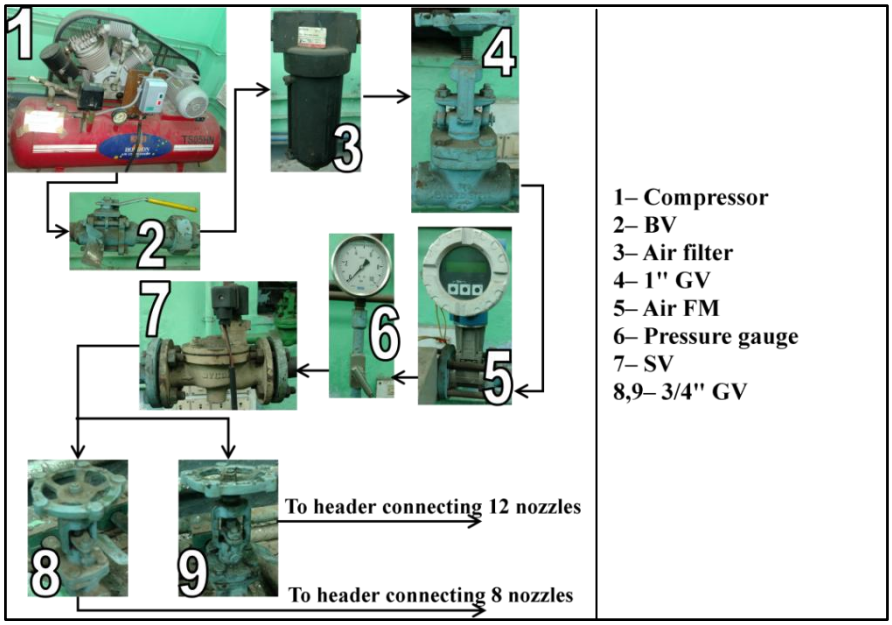

Fig.2.3: Air Circuit

Table.2.3: Specifications of air line components

Component	Qty.	Make	Model	Specification
Compressor	1	ELGI Equipments Ltd.	TS05 120 H	Unit RPM: 925 Max. Working Pressure: 12kgf/cm^2 Air Receiver Capacity: 220L Motor Used: ELGI made, 5.5hp, 1450rpm, 50Hz
Ball Valve (BV)	1	Mevada Engineering Works (P) Ltd.	BL-30-F-W-A3	Size and Rating: 1", S.W. 600#
Air Filter	1	ShavoNorgen	SF17-800-M8DC	Size and Rating: 1", BSP(F) 800# Max. Inlet Pressure: 17.5kgf/cm^2
Vortex Flow Meter	1	Endress + Hauser	PROWIRL 72W 25	Size: 1", 150#, FLGD Max. Flow: 10m^3/h Max. Pressure: 8bar Supply: 24V DC
Pressure Gauge	1	Wika	EN837-1	Range: 0-10bar Size: ½" BSP(M)
Needle Valve	1	Expo Engineering Enterprises	E8-NVFN	Size and Rating: ½", BSP(F), 800# (TH)
Solenoid Valve (SV)	1	Avcon	9160K25/CI/S4/ BN/A1	Size and Rating: 1", FLGD, 150# Supply: 24V DC
Globe Valve (GV)	1	Mevada Engineering Works (P) Ltd.	GB-1-R-W-A4	Size and Rating: 1", S.W. 800#
	2			Size and Rating: ¾", S.W. 800#

Water supply comes from an overhead tank and goes into a simplex basket filter first through a BV. Then a vertical inline multistage centrifugal pump pressurizes the water and delivers it through a pressure gauge, fitted with a needle valve. The line divides then into a bypass line and main line after that. The bypass line contains a normally open pilot operated diaphragm type SV and a 1"GV to regulate and control the water flow. From Fig.2.4 it can be seen that, the main line gets divided into two branches after another filtration. Each of the lines contains a normally closed SV and a flow meter. The line which has larger diameter goes to the mist spraying nozzles and the other line goes to the water spraying nozzles. Both lines are provided with a GV and a pressure gauge each. Each line again divides into two lines to supply water to the headers connecting 8 nozzles and 12 nozzles separately as in Fig.2.4. Globe valves are provided to control flow in every line to the headers. Table.2.4 contains the specifications in detail. In the present circumstances though, the water supply line is not used as only air-cooling has been studied.

The electro-hydraulic actuation system consists of a power pack, a proportional valve (PV) and a hydraulic actuator. Hydraulic oil of grade Servo system HLP 68 is used. Oil goes from the reservoir to a swash plate type axial piston pump, driven by a 3-phase induction motor, through an oil filter. A pressure relief valve (PRV), connected to the line, limits the maximum line pressure. The oil goes to the PV which is a solenoid operated 4-way 3-position direction control valve. This valve drives a single acting actuator, which is hinged to a mechanical link, connected to a rod protruding from the holding tray as shown in Fig.2.5. The pin joint at the fulcrum point of the link divides it at a ratio 1:4 from the actuator end to the rod end, making the speed of the plate four times of the actuator speed. The stroke lengths of the cylinder and the plate are also in the same ratio. The actuator displacement is fed back to the real-time system with the help of an LVDT. The compact-reconfigurable input–output real-time system (cRIO RTS), consisting of a 16-bit NI-cRIO 9102 real-time serial processor with digital to analog and analog to digital signal converter, an NI-cRIO 9004 real-time controller, an NI-cRIO 9215 input module and an NI-cRIO 9263 output module, serves as the data acquisition system, interfaced through a Host PC, which sends signal to a valve-control card (VCC), having 0.04% gain error, through the output module of the RTS. The VCC in turn directs command voltage to the PV. There is also an NI-cRIO 9211 input module for temperature input in the data acquisition system so that the same can be used for determining the temperature of the heated plate as well. Detailed specifications are given in Table.2.5.

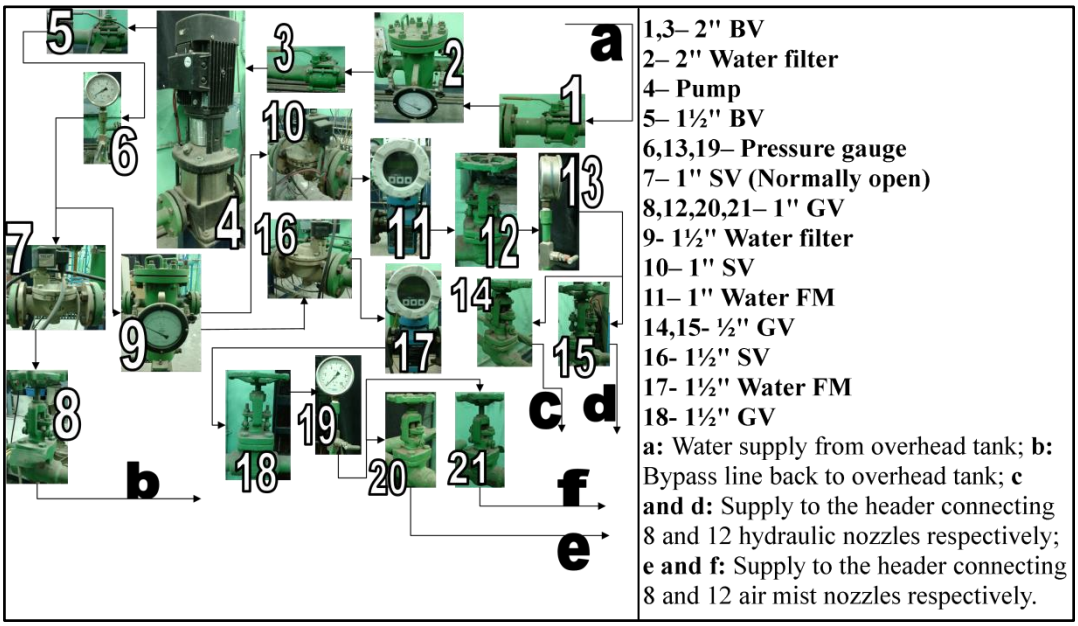

Fig.2.4: Water Circuit

Table.2.4: Specifications of water line components

Component	Qty.	Make	Model	Specification
Water Filter	2	Filtration Engineers India Pvt. Ltd.	FR-244450NB	Size and Rating: 2", ANSI FLGD, 150# Mesh: 200µ Max. Pressure: 2bar
			FR-244440NB	Size and Rating: 1 ½", ANSI FLGD, 150# Mesh: 100µ Max. Pressure: 5bar
Ball Valve (BV)	2	Mevada Engineering Works (P) Ltd.	BL-30-F-W-A3	Size and Rating: 2", S.W.600#
	1			Size and Rating: 1 ½", S.W.600#
Pump	1	Grundfos	CR10-4-A-FJ-A-E-HQQE	RPM: 2896 Max. Flow: 10m^3/h Shut Off Head: 40.8m Motors used: (a) Grundfos made, 1.5kW, 50Hz, 2890-2910rpm (b) Grundfos made, 1.5kW, 60Hz, 3470-3530rpm
Pressure Gauge	3	Wika	EN837-1	Size: ½", BSP(M) Range: 0-10bar
Needle Valve	3	Expo Engineering Enterprises	E8-NVFN	Size and Rating: ½", BSP(F), 800# (TH)
Solenoid Valve (SV)	1	Avcon	9162K25/CI/S4/BN/A1	Size and Rating: 1", FLGD, 150# Supply: 24V DC
	1		9160K25/C1/S4/BN/A1	
	1		9160K35/C1/S4/BN/A1	Size and Rating: 1 ½", FLGD, 150# Supply: 24V DC
Electromagnetic Flow Meter	2	Endress + Hauser	PROMAG 10P 25	Size: 1", FLGD, 150# Max. Flow: 10m^3/h Max Pressure: 10bar Supply: 220V AC 50Hz
				Size: 1 ½", FLGD, 150# Max. Flow: 10m^3/h Max Pressure: 10bar Supply: 220V AC 50Hz
Globe Valve (GV)	4	Mevada Engineering Works (P) Ltd.	GB-1-R-W-A4	Size and Rating: 1", S.W. 800#
	1			Size and Rating: 1 ½", S.W. 800#
	2			Size and Rating: ½", S.W. 800#

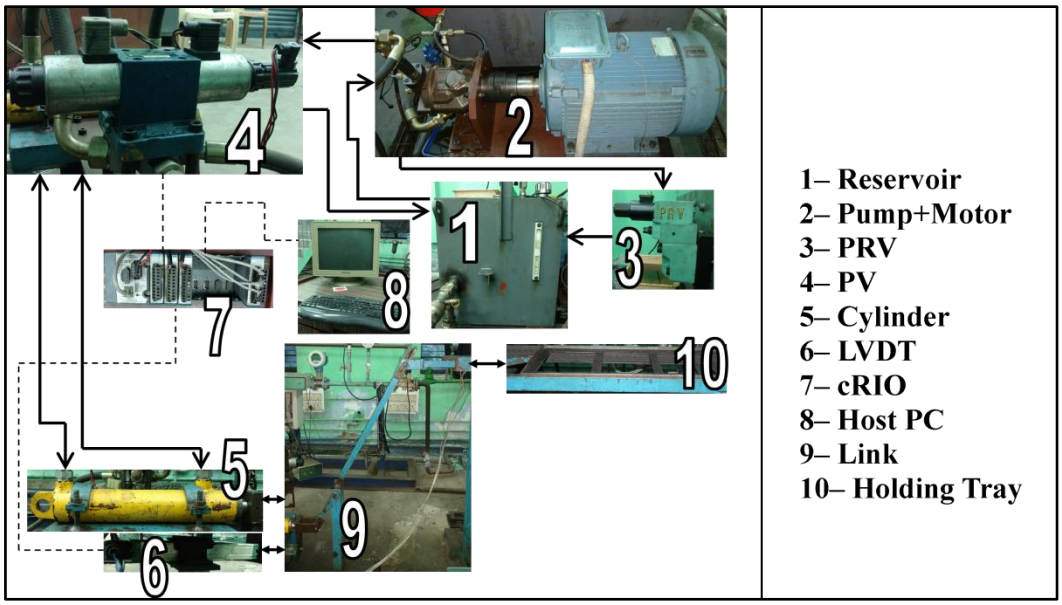

Fig.2.5: Electro-Hydraulic Actuation System (EHAS)

Table.2.5: Specifications of the components of the EHAS

Component	Qty.	Make	Model No.	Specification
Pump	1	Rexroth	A10VSO 45DR/31 R-PPAI2NOO	Nominal Pressure: 280bar Flow: 60Lpm Motor Used: ABB made, 30kW, 50Hz, 1470rpm
PRV	1	Yuken	EBG-03-H-11	Max. Pressure: 245bar
Oil Filter	1	Hydac	DFBN/HC110G10B 1.1	Max. Pressure: 420bar
PV	1	Rexroth	4WRE 10 E1-50-21/G24K4/V	Flow: 50Lpm Supply: 24V DC Deadband: ±1.5V Solenoid Resistance: 4.1Ω Solenoid Input Current: 2.6A
Actuator	1			Type: Single acting Bore: 50mm Stroke length: 200mm
LVDT	1	Gefran	LT-M-0200S-XL02020000X000X00	Stroke Length: 200 mm Linearity: ±0.05% Repeatability: 0.01 mm
Real-time serial processor	1	National Instruments	NI-cRIO-9102	16-bit, 1kHz sampling rate, Accuracy: ±100ppm(max)
Input Module	2	National Instruments	NI-cRIO-9215	4-Ch ±10V 16 bit simultaneous analog input Max. Gain Error: 0.2%
			NI-cRIO-9211	4-Ch ±80mV 24 bit thermocouple input Max. Gain Error: 0.05% at 25°C
Output Module	1	National Instruments	NI-cRIO-9263	4-Ch ±10V 16 bit analog output Max Gain Error:0.35%

There are two holding trays for the sample plate. One tray that is used in the furnace while heating the and the other one, attached to the mechanical link connected to the actuator, is the tray used for reciprocation.

Two MS plates of dimensions 597×202×10mm and 597×202×6mm have been used in the experiments as sample plates. These sample plates have been drilled at the required locations and four K-type thermocouples have been attached to that.

The thermocouples have been attached to four locations of the sample MS plate. At first, the sample plate is heated in the furnace up to desired temperature, which is called the target temperature. PID controller has been used to control the target temperature so that the heater stops automatically on reaching the target. The heated plate is drawn out from the furnace manually and dragged to the cooling bay upon the roller fitted rails. The ball valve of the airline is opened prior to the starting of the compressor. The two ¾" GVs, which lead directly to the nozzle bank headers, have been equally opened to ensure same velocity of air jet through each of the nozzles. The main GV of 1" NB is opened or closed gradually to increase or decrease the air flow rate (Q) respectively as per requirement. The flow meter reading has been observed and the GV is set at desired flow rate. The nozzle banks are set at desired distance (D) from the cooling bay with the help of the adjustment wheel during heating of the plate. The solenoid valve has been energized to open and allow air flow through it and the data acquisition process has also been started at the same time by running the VI on LabVIEW in the Host PC. The instantaneous temperatures (T) at four locations of the plate have been recorded with a time step of 0.01sec by the RTS during the whole cooling process and the average of the four has been determined to get the average plate temperature (T_{avg}). When the plate reaches the room temperature of 30^{o}C, the data acquisition is stopped with the compressor turned off. The same process is repeated changing any of the parameters among flow rate (Q), initial temperature of the plate (T_{in}) and nozzle bank distance (D). The results and the observations have been detailed in the following chapter.

Chapter 3

Results and Discussions

The cooling features of the sample plate have been studied in real-time using the system described in Chapter 2. Three parameters, i.e. Air Flow Rate (Q) from the nozzles, Initial Temperature of the sample plate (T_{in}) and Nozzle Bank Distance (D) from the plate, have been varied and cooling behaviour of the plate is studied over different conditions. Equivalent sets of experiment have been carried out on two Mild Steel sample plates having different thicknesses of 6mm and 10mm.All the nozzles have been kept open and the plate has been cooled to room temperature (30^oC) in each run.

In each run one of the above mentioned three parameters has been treated as variable and the other two have been kept constant at some pre-determined base value. For example, while studying the effect of change of Q on the cooling of the plate, T_{in} and D have been kept fixed at their base values. Ranges and base values of the parameters have been given in Table.3.1. For each parameter the base value has been chosen somewhere around the midpoint of the range. The instantaneous temperatures (T) during cooling of the sample plate have been recorded by the RTS at four locations of the plate and sample plots of the same with time (t) for two plates have been shown in Fig.3.1.In each of these two real time plots four T readings have been plotted simultaneously against time with all the parameters set at their respective pre-determined base values. From Fig.3.1 it can be seen that the four readings differ negligibly from each other. So, it is reasonable to make the assumption that the plate temperature is almost uniform and average of the four temperature readings (T_{avg}) can be taken to represent the plate temperature as a whole.

Table.3.1: Ranges and base values of the parameters

Parameter	**Range**	**Base Value**
Flow Rate (Q)	5-7m^3/h	6m^3/h
Initial Temperature of the plate (T_{in})	100^{o}C-700^{o}C	300^{o}C
Nozzle bank distance (D)	45-185mm	115mm

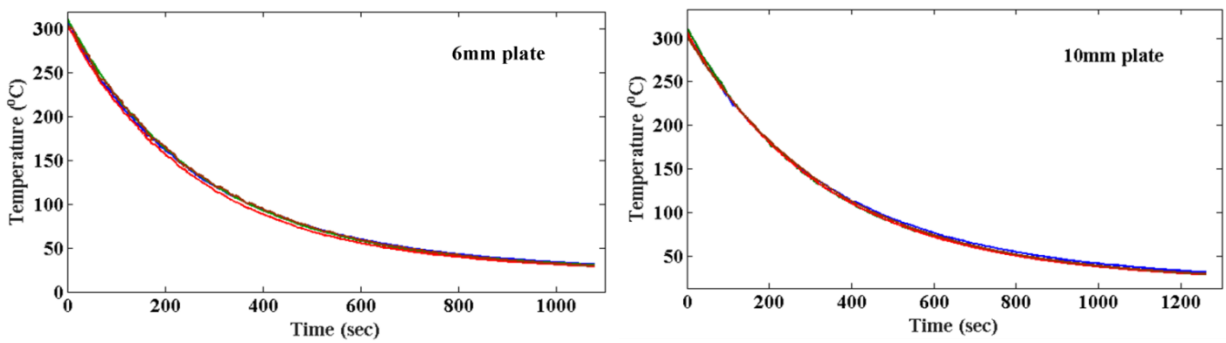

Fig.3.1:Real-time temperature plot with all parameters set at their respective base values

The heat transfer coefficient (h) has been calculated from the convection equation of the plate while making a few assumptions to simplify the calculation. From the physical situation of the plate it can be said that convection is the major mode of heat transfer from the plate during cooling, in comparison of which contribution of radiation and conduction can be neglected. Apart from that the plate is assumed to be thin and so, zero heat loss from all the surfaces except those directly under air jet can be assumed. The recorded data have shown that spatial variation of temperature over the plate to be negligible. Thus, the plate has been assumed as a lumped system and uniform temperature is assumed all over the plate. So, with the assumptions stated above, h can easily be calculated from the convection equation, which reduces to the following simple form due to those assumptions:

$$hA(T - T_{\infty}) = mc_p\left(\frac{dT}{dt}\right) \quad \textbf{(1)}$$

Where, A= Surface Area (the total area of the two surfaces under air jet)

T_{∞}= Ambient Temperature (taken to be 30^{o}C)

m= mass of the plate

c_p= specific heat of Mild Steel

Now, $\left(\frac{dT}{dt}\right)$in (1) is basically the temperature gradient or the cooling rate, which can be obtained from T readings. Standard values have been assumed for density (ρ = 7850kg/m^3) and specific heat (c_p = 510.7896J/kg-^{o}C) of mild steel. Plots of the average temperature (T_{avg}), the cooling rate (θ) and the heat transfer coefficient (h) against time (t) have been obtained for different conditions.

❖ ***Effect of change of flow rate***

The effect of air flow rate (Q) on the cooling behaviour of the plate has been studied by taking the temperature readings at three different flow rates for both of the plates. Table.3.2 contains the brief details of the parameter settings used. The parameters have been changed in consecutive runs to observe the change in cooling behaviour while the rest of the parameters have been kept constant at their base values mentioned in Table.3.1.

Table.3.2: Experimental runs to study the effect of flow rate

Run	Flow Rate, Q (m^3/h)	Average flow velocity from nozzles, (m/s)
1	5	17
2	7	26
3	6	21

Fig.3.2 shows the corresponding cooling behaviour from where it can be clearly seen that the thicker plate has required almost 5minutes more time to cool to the room temperature than the other plate. The slope of the temperature curve decreases gradually and the curve flatens more and more as time goes on. This happens because the temperature difference between the plate and the surroundings decreases as it cools down. In the near room temperature zone the temperature difference between the plate and the surroundings almost becomes zero. Thus the curve shows asymptotic behaviournear the end. From the plots it is clear that cooling gets better and faster for higher Q, which is quite obvious.

Cooling rates (θ) of the sample plates have been expressed in the unit of ^{o}C/sec. It is basically the gradient or slope of the average temperature curves obtained. As discussed earlier temperature gradient decreases gradually as time goes on. Fig.3.3 reveals the same fact as we can see that the θ - t curves almost tend to zero near the end when T_{avg} approaches the room temperature. Getting higher θ for higher Q is expected naturally and also happens to be indicated by the curves.

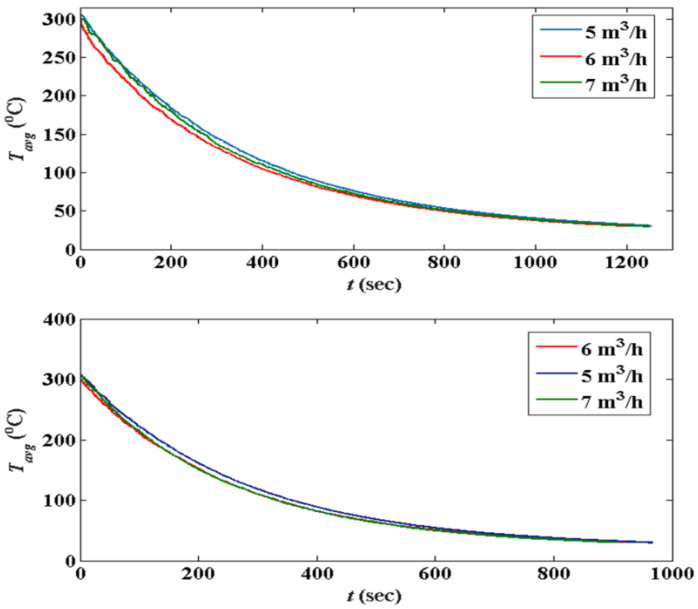

Fig.3.2: Plot of average temperature for different flow rates

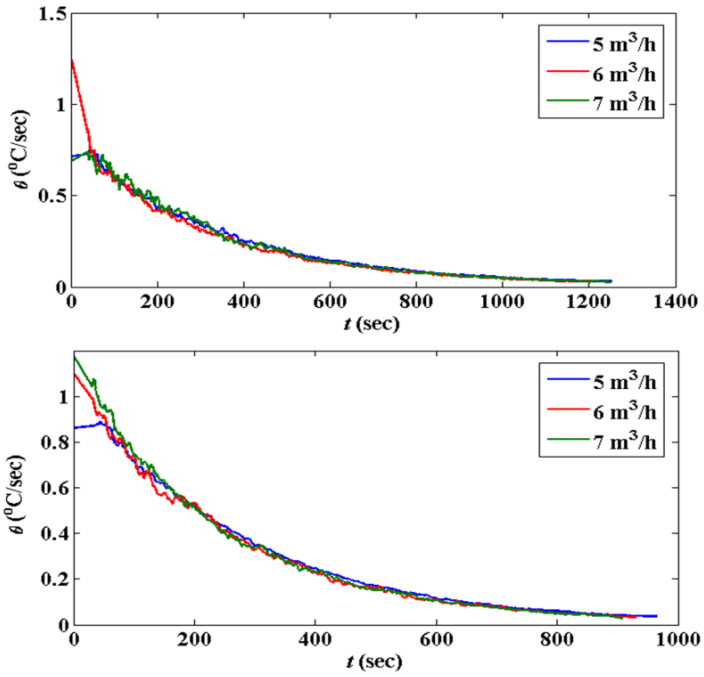

Fig.3.3: Plot of cooling rate for different flow rates

The changes in the heat-transfer co-efficients (*h*) with time,corresponding to the three different *Q*, have been plotted Fig.3.4.It can be seen clearly that heat transfer coefficientis more for the 10mm plate than the 6mm plate. This is because the heat capacity of the 10mm plate is more than that of the 6mm plate. Both the curves show very slow increment in *h*at the beginning. The gradient of the curve is almost zero upto the first 6.5 minutes of cooling for the 6mm plate and for the 10mm plate that is upto first 10minutes of cooling. For the cases *h*remains almost constant respectively at approximately 50W/m^2-^{o}C and 60W/m^2-^{o}C. Itincreases gradually after that for both curves. From Fig.3.3 it has been seen θ becomes almost constant after reaching a certain point of time for both the cases but however slow it may be, the temperature difference between the plate and the surrounding keeps on decresing. From (1), it can be easily seen that if θ remains constant and the temperature difference decreases, *h*will certainly increase. Slope of the curves keep on increasing slowly at first, but near the end it increases rapidly for both cases. The heat transfer coefficient shoots up to its maximum value very rapidly at the terminating region of cooling for both the plates. Taking any of the plates into account we can see that the maximum value of *h*does not depend that much on the value of *Q* and it is higher for the 10mm plate.

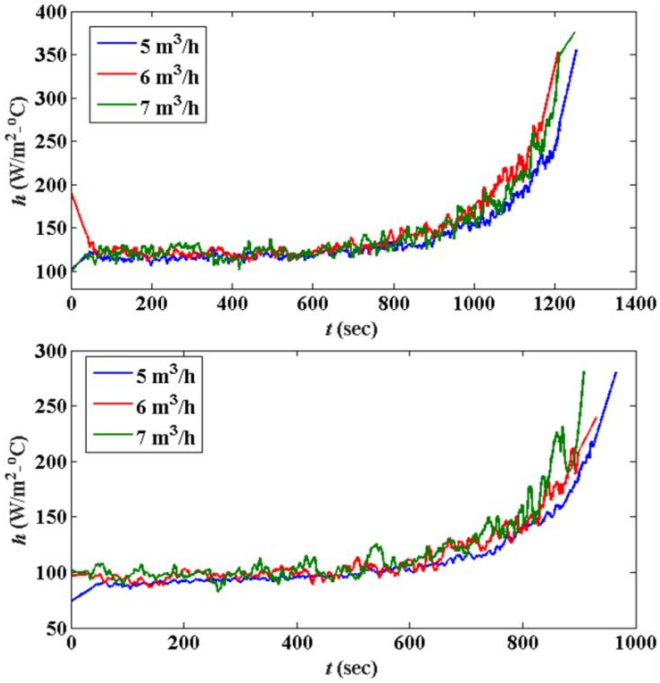

Fig.3.4: Plot of heat transfer coefficient with different flow rates

❖ ***Effect of change of Initial Temperature of the plate***

Initial Temperature (T_{in}) of the plate refers to the temperature at the start of cooling. Table.3.3 contains the details of the experimental runs. The other parameter values have been kept at the base values mentioned in Table.3.1.

Table.3.3: Experimental runs to study the effect of initial temperature

Run	Initial Temperature of the plate, T_{in} (^{o}C)
1	600
2	500
3	400
4	300
5	200
6	100

T_{avg}, Q and θ are plotted against time for different T_{in} in Figs.3.5-3.7. Trends of all the curves match with the general perception of higher the T_{in}, longer it will take to get cooled to room temperature.

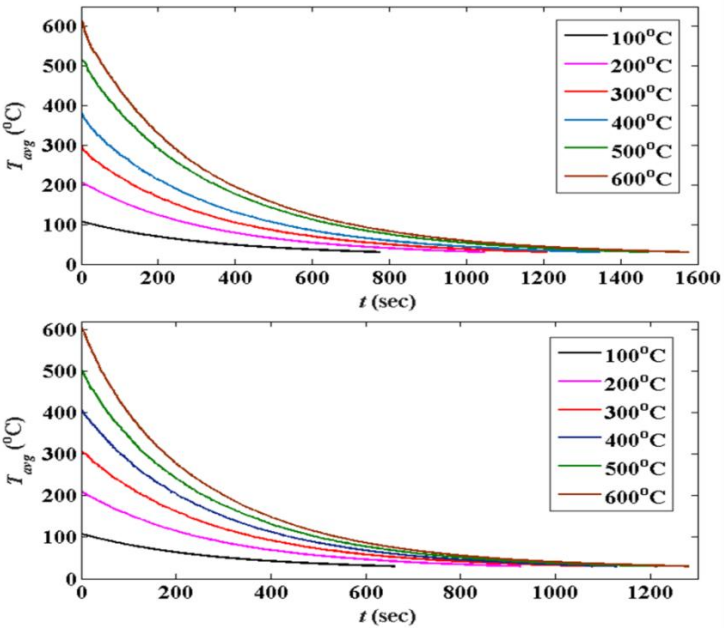

Fig.3.5: Plot of average temperature with different initial temperature values

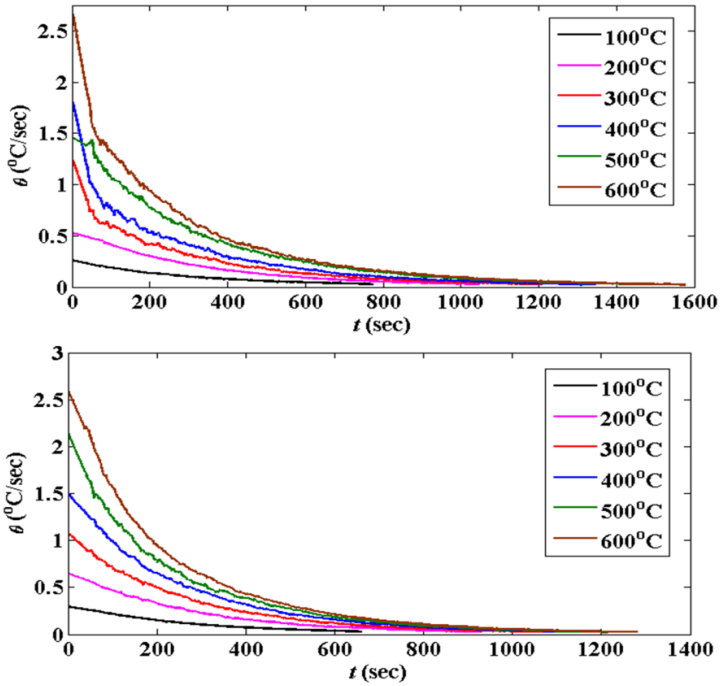

Fig.3.6: Plot of cooling rate with different initial temperature values

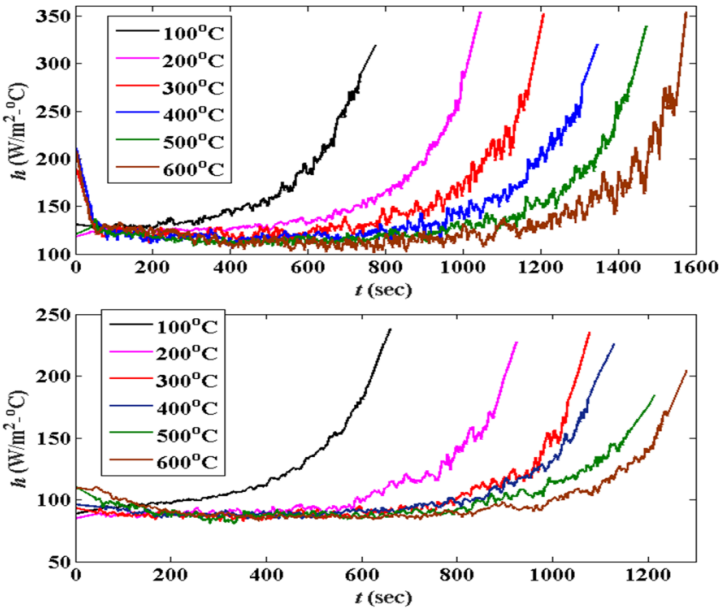

Fig.3.7: Plot of heat transfer coefficient with different initial temperature values

❖ ***Effect of change of Nozzle Bank Distance***

Cooling behaviour of the plate changes interestingly with change in Nozzle Bank Distance (*D*). On both sides of the plate the respective nozzle banks have been kept at same distance from the plate, and that distance has been referred to as the Nozzle Bank Distance (*D*) from the plate in this analysis.In Table.3.4 below, values of *D* for each run are given while the other parameters are again kept at their base values mentioned in Table.3.1. The cooling behaviour is shown in Fig.3.8.

Table.3.4: Experimental runs to study the effect of nozzle bank distance

Run	Nozzle bank distance from plate, *D* (mm)
1	55
2	85
3	115
4	145
5	175

Air jet after coming out from the nozzle diverges. Thus the air jet velocity at the moment of hitting the plate diminishes gradually as the nozzle is moved further from the plate beacuse air jet from the nozzle has to cover more distance to reach the plate. For sake of convenience the velocity with which the air jet hits the plate, can be called as incident velocity.

Now, the convective heat transfer is more for higher incident velocity as more heat will be swept at a time away with higher velocity. So, convective heat transfer gets better with decreasing *D*. The small area on the plate that comes directly under the purview of air jet can be called effective area under cooling of that nozzle. But, as the nozzle bank is moved closer to the plate

thatarea reduces. Conductive heat transfer from the adjoining areas, which are still comparatively hotter than the effective area of cooling, helps to transmit the cooling effect throughout the plate. But heat removal is more and faster for convection than conduction. So, to increase the convective component in cooling, the effective area under direct cooling of air jet has to be increased. Having multiple jets boosts the convective cooling to a great extent but still there will be some areas that are not coming under the air jet cooling directly and have to rely more on conduction for getting cooled. Moving the nozzle bank further can certainly increase the effective area of the plate coming under the air jet from the nozzle as the jet is a divergent one. Thus convective cooling will enhance and dependence on conductive cooling will reduce. So, two opposing effects can be seen here. In order to obtain minimum cooling time, *D* must be set at some intermediate value between the maximum and the minimum. Table.3.5 compares the required cooling times for various nozzle settings for both the plates.From the table so also from Fig.3.8, it can be seen that the plate takes least time to cool down to room temperature when the nozzle bank distance is set at 85mm. That means 85mm is the optimal setting for the nozzle banks.

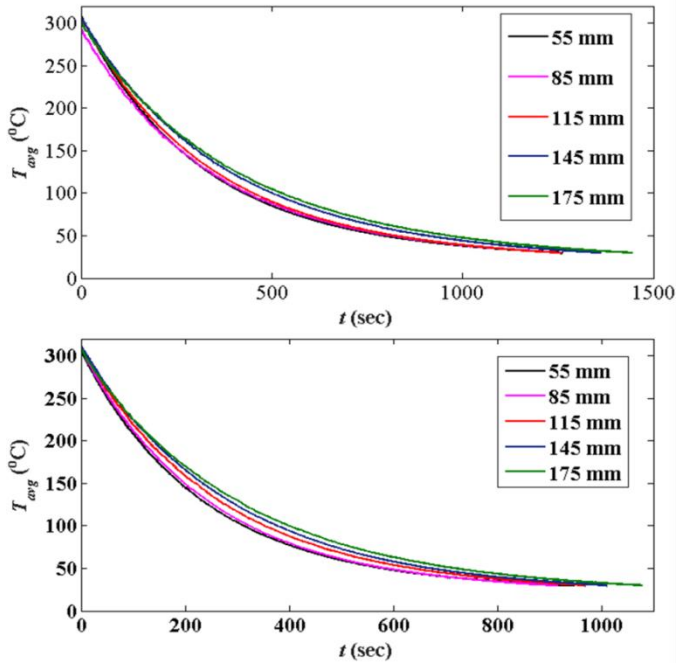

Fig.3.8: Plot of average temperature with different nozzle bank distances

Table.3.5: Comparison of cooling time for various nozzle bank positions

Nozzle Bank Distance (mm)	For 6 mm plate	For 10 mm plate
	Cooling Time (sec)	Cooling Time (sec)
55	949	1263
85	**917**	**1239**
115	970	1261
145	1011	1364
175	1078	1446

From the plot of the cooling rates (θ) in Fig.3.9, we can infer that, at the initial stage of cooling when θ is high and reducing rapidly, it is clear that for nozzle bank distance of 55mm, θ is maximum, followed by those for 85mm, 115mm, 145mm and 175mm nozzle bank distances respectively. From the trend in this zone of cooling it can be concluded that to have higher θ, D has to be lowered. So, θ and D are related inversely in this zone. This trend prevails upto approximately 100^{o}C of T_{avg}. When the plate is cooled beyond 100^{o}C the trend of cooling reverses its nature. In this zone of low θ and slow cooling, θ is found to be maximum for 175mm of D, followed by that for 145mm, 115mm, 85mm and reach the minimum for 55mm of the nozzle bank distance. So in this zone θ and D are related directly, which is just the opposite of the situation that prevails before 100^{o}C. This intriguing observation can be explained by analysing the physical situation carefully. It has been already elaborated how the relation between convective heat transfer and D depends majorly on two opposing factors, incident velocity of the air jet and effective area under direct cooling of the air jet. Individual increment in any of these two factors can surely enhance convective heat transfer upto some limit if the other factor can be held at a constant value. But in this case, the two factors are dependent on each other. Moving the nozzle bank further away will increase the effective area under direct cooling of the air jet and thus should increase convective heat transfer. But the incident velocity will decrease with the nozzle bank moving away from the plate and thus will lower the amount of convective heat transfer. Similarly moving the nozzle bank closer to the plate will increase the incident velocity which in turn should boost up convection but on the other hand smaller effective area under direct cooling will increase the dependenceon conduction. Now the whole cooling process can be divided in two zones with opposite trends of cooling, high temperature zone (T_{avg} above 100^{o}C) and low temperature zone (T_{avg} below 100^{o}C). For 6mm plate the high temperature zone spans approximately upto 355sec from the start and for 10mm plate this zone spans approximately upto 480sec from the start of cooling.

Now, in the high temperature zone the effect of the incident velocity on convective cooling is predominant over the effect of the effective area under direct cooling because the temperature difference in this zone is higher. As the temperature difference is higher, cooling is rapid in this zone. So, convection performs better comparatively than low temperature zone. Now in this zone if the nozzle bank is set close to the plate, higher incident velocity enhances convection and smaller effective area under direct cooling poses a challenge for convection and the cooling process has to depend on conduction within the plate. Due to high θ the temperature drop at a time of the effective area under direct cooling is also high. Thus rate of conduction between the directly jet cooled area and the adjoining comparatively hot areas is also high. As the rate of conduction is very high it successfully supplements the reduction in convective cooling. Because of that the effect of the effective area under direct cooling on the process practically becomes intangible. Thus the effect of the effective area under direct cooling is majorly predominated by the effect of incident velocity in

high temperature zone of cooling. So the incident velocity is the determining factor of the relation between θ and D in this zone. Due to that fact lowering D will increase θ consistently in this zone. This trend reflects very clearly in the above experimental results.

In the low temperature zone below 100^{o}C, the temperature difference between the plate and the surroundings is low. From the T_{avg} plots it can be seen that after crossing the 100^{o}C mark convective cooling almost reaches its saturation and the rate of cooling from there on is quite low. In this zone increasing the incident velocity of the air jet does not significantly increase the rate of forced convection. As the rate of convective cooling is low, temperature drop at a time is low in the effective area under direct cooling. Thus rate of conduction within the plate also becomes very low. When the nozzle bank is lowered from higher postion, the increment in incident velocity fails to leave any significant mark on the rate of convection whereas due to smaller effective area under direct cooling the rate of cooling reduces signifantly as the low rate of conduction cannot supplement the reduction in convective cooling anymore. So, as a whole θ reduces with lowering of D. It can thus be said that in the lower temperature zone effect of the effective area under direct cooling of air jet predominates over the effect of incident velocity of air jet. That is why in this zone the effective area under direct cooling practically becomes the deciding factor of the relationship between θ and D. As the nozzle bank is moved further away from the plate, cooling rate increases. This trend can be seen exactly in the results too.

The plot of h in Fig.3.10 clearly indicates the co-efficient to have higher value for smaller D and it takes more time for higher D to reach maximum h value.

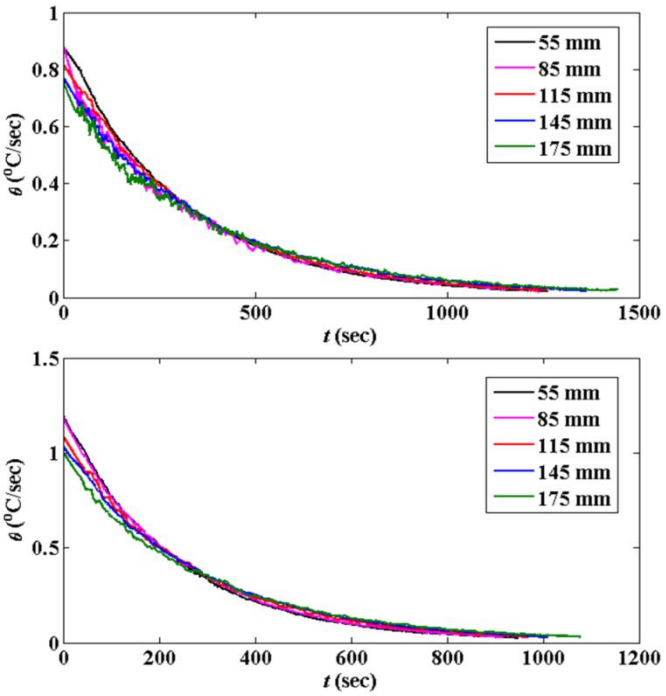

Fig.3.9: Plot of cooling rate with different nozzle bank distances

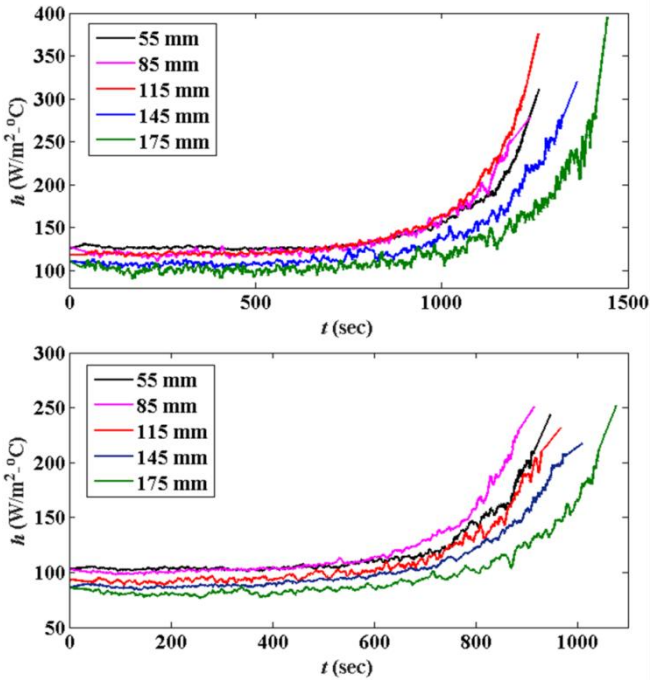

Fig.3.10: Plot of heat transfer coefficient for different nozzle bank distances

❖ ***Pridicting the nature of relationship between average temperature and individual parameters***

The functional relationship between average temperature (T_{avg}) and each individual parameter has been attempted to find. MATLAB surface fitting tool has been used to obtain the surface plots with T_{avg} on the *z* axis and time (*t*) on the *y* axis, and the three parameters, i.e. flow rate (*Q*), initial temperature (T_{in}) and nozzle bank distance (*D*), plotted on the*x* axis one at a time. From each of those surface plots average temperature can be established as a function of time and the other parameter.

From the surface plots given below in Fig.3.11,average temperature can be expressed as a polynomial function of flow rate and timeas,

$$T_{avg}(Q,t) = p_{00} + p_{10}Q + p_{01}t + p_{11}Qt + p_{02}t^2 + p_{12}Qt^2 + p_{03}t^3 + p_{13}Qt^3 + p_{04}t^4 + p_{14}Qt^4 + p_{05}t^5 \quad \textbf{(2)}$$

The polynomial, which is 1st order for *Q*and 5th order in *t*, is chosen on the basis of the trend of the experimental results.

Coefficients of (2) and the statistics measuring goodness of the fit are given in Table.3.6 and Table.3.7 respectively for the plates of 10mm and 6mm thicknesses.

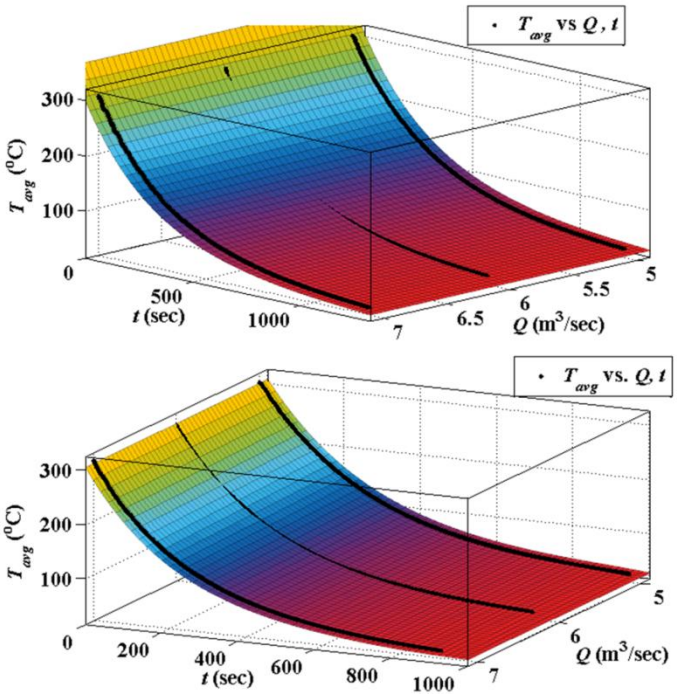

Fig.3.11: Surface plot of average temperature vs. flow rate and time

Table.3.6: Coefficients of (2) and Goodness of Fit Statistics for 10mm Plate

Coefficients (with 95% confidence bounds)	
p_{00}	70.27 (70.25, 70.3)
p_{10}	-1.543 (-1.565, -1.521)
p_{01}	-47.01 (-47.06, -46.95)
p_{11}	1.245 (1.215, 1.274)
p_{02}	22.71 (22.66, 22.75)
p_{12}	0.1125 (-0.1577, -0.06737)
p_{03}	-8.348 (-8.414, -8.282)
p_{13}	-0.3812 (-0.3958, -0.3666)
p_{04}	2.996 (2.979, 3.012)
p_{14}	0.1406 (0.1242, 0.1571)
p_{05}	-0.662 (-0.6811, -0.6429)
Goodness of fit	
R-square*	0.9974
Adjusted R-square†	0.9974

*R-Square measures how successful the fit is in explaining the variation of the data. R-square can take on any value between 0 and 1, with a value closer to 1 indicating that a greater proportion of variance is accounted for by the model. If you increase the number of fitted coefficients in your model, R-square will increase although the fit may not improve in a practical sense. To avoid this situation, you should use the degrees of freedom adjusted R-square statistic.

†Degrees of Freedom Adjusted R-Square uses the R-square statistic defined above, and adjusts it based on the residual degrees of freedom. The residual degrees of freedom is defined as the number of response values minus the number of fitted coefficients estimated from the response values. The adjusted R-square statistic can take on any value less than or equal to 1, with a value closer to 1 indicating a better fit.

[Source: Goodness-of-Fit Statistics, Residual Analysis, Curve Fitting Technique, User's Guide, Curve Fitting Toolbox, *MATLAB 7.12.0.635 (R2011a) Product Help*, MathWorks]

Table.3.7: Coefficients of (2) and Goodness of Fit Statistics for 6mm Plate

Coefficients (with 95% confidence bounds)	
p_{00}	70.26 (70.25, 70.28)
p_{10}	-2.214 (-2.226, -2.202)
p_{01}	-48.49 (-48.52, -48.46)
p_{11}	1.939 (1.923, 1.956)
p_{02}	24.36 (24.34, 24.39)
p_{12}	-0.732 (-0.7574, -0.7067)
p_{03}	-8.567 (-8.604, -8.53)
p_{13}	-0.6498 (-0.6583, -0.6413)
p_{04}	2.576 (2.566, 2.585)
p_{14}	0.4374 (0.4279, 0.4468)
p_{05}	-0.4987 (-0.5094, -0.488)
Goodness of fit	
R-square	0.9993
Adjusted R-square	0.9993

From Fig.3.12, average temperature can be expressed as a polynomial function of initial temperature of the plate and time as,

$$T_{avg}(T_{in}, t) = p_{00} + p_{10}T_{in} + p_{01}t + p_{11}T_{in}t + p_{02}t^2 + p_{12}T_{in}t^2 + p_{03}t^3 + p_{13}T_{in}t^3 + p_{04}t^4 + p_{14}T_{in}t^4 + p_{05}t^5 \quad \textbf{(3)}$$

The polynomial, which is 1st order for T_{in} and 5th order in t, is chosen on the basis of the trend of the experimental results. Coefficients of (3) and the statistics measuring goodness of the fit are given in Table.3.8 and Table.3.9 respectively for the plates of 10mm and 6mm thicknesses.

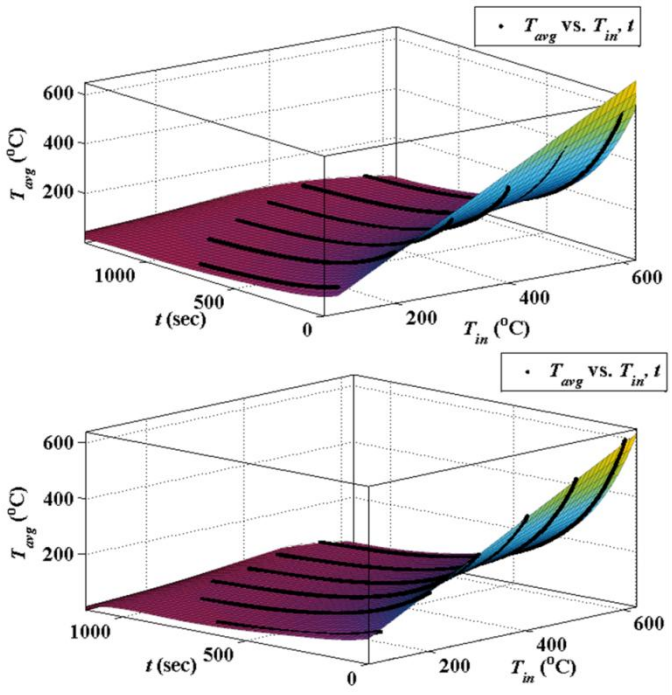

Fig.3.12: Surface plot of average temperature vs. initial temperature and time

Table.3.8: Coefficients of (3) and Goodness of Fit Statistics for 10mm Plate

Coefficients (with 95% confidence bounds)	
p_{00}	79.18 (79.16, 79.2)
p_{10}	26.13 (26.11, 26.15)
p_{01}	-61.33 (-61.37, -61.28)
p_{11}	-23.55 (-23.58, -23.51)
p_{02}	30.76 (30.71, 30.81)
p_{12}	13.12 (13.06, 13.17)
p_{03}	-12.27 (-12.33, -12.21)
p_{13}	-9.31 (-9.33, -9.289)
p_{04}	7.122 (7.099, 7.144)
p_{14}	3.35 (3.329, 3.37)
p_{05}	-2.328 (-2.345, -2.31)
Goodness of fit	
R-square	0.9971
Adjusted R-square	0.9971

Table.3.9: Coefficients of (3) and Goodness of Fit Statistics for 6mm Plate

Coefficients (with 95% confidence bounds)	
p_{00}	76.32 (76.31, 76.34)
p_{10}	21.64 (21.63, 21.66)
p_{01}	-61 (-61.03, -60.96)
p_{11}	-21.27 (-21.29, -21.24)
p_{02}	31.99 (31.95, 32.03)
p_{12}	10.88 (10.85, 10.92)
p_{03}	-12.18 (-12.22, -12.14)
p_{13}	-10.3 (-10.32, -10.29)
p_{04}	8.551 (8.535, 8.567)
p_{14}	4.722 (4.707, 4.737)
p_{05}	-3.371 (-3.384, -3.358)
Goodness of fit	
R-square	0.9991
Adjusted R-square	0.9991

From Fig.3.13, average temperature can be expressed as a polynomial function of nozzle bank distance from the plate and time as,

$$T_{avg}(D,t) = p_{00} + p_{10}D + p_{01}t + p_{20}D^2 + p_{11}Dt + p_{02}t^2 + p_{30}D^3 + p_{21}D^2t + p_{12}Dt^2 + p_{03}t^3 + p_{31}D^3t + p_{22}D^2t^2 + p_{13}Dt^3 + p_{04}t^4 + p_{32}D^3t^2 + p_{23}D^2t^3 + p_{14}Dt^4 + p_{05}t^5 \quad \textbf{(4)}$$

The polynomial, which is 3rd order for *D*and 5th order in *t*, is chosen on the basis of the trend of the experimental results.

Coefficients of (4) and the statistics measuring goodness of the fit are given in Table.3.10 and Table.3.11 respectively for 10mm and 6mm plate.

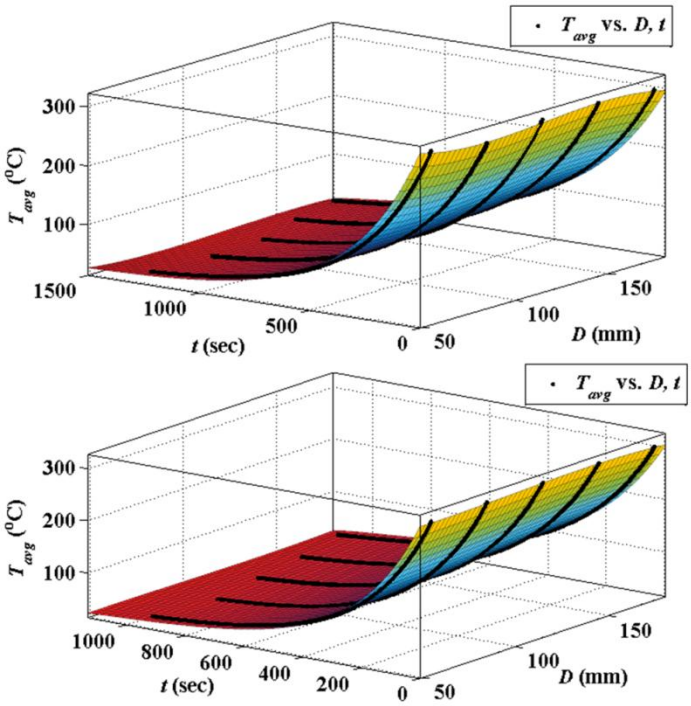

Fig.3.13: Surface plot of average temperature vs. nozzle bank distance and time

Table.3.10: Coefficients of (4) and Goodness of Fit Statistics for 10mm Plate

Coefficients (with 95% confidence bounds)	
p_{00}	67.92 (67.92, 67.93)
p_{10}	7.537 (7.526, 7.547)
p_{01}	-47.02 (-47.03, -47.01)
p_{20}	1.543 (1.539, 1.548)
p_{11}	-6.422 (-6.431, -6.414)
p_{02}	23.67 (23.66, 23.68)
p_{30}	-0.5832 (-0.589, -0.5774)
p_{21}	0.3658 (0.3585, 0.373)
p_{12}	1.302 (1.29, 1.313)
p_{03}	-9.093 (-9.104, -9.081)
p_{31}	1.758 (1.754, 1.762)
p_{22}	-0.5666 (-0.57, -0.5633)
p_{13}	1.368 (1.365, 1.371)
p_{04}	3.17 (3.166, 3.173)
p_{32}	-1.192 (-1.197, -1.188)
p_{23}	0.1442 (0.1404, 0.148)
p_{14}	-0.3932 (-0.3968, -0.3895)
p_{05}	-0.652 (-0.6554, -0.6486)
Goodness of fit	
R-square	0.9998
Adjusted R-square	0.9998

Table.3.11: Coefficients of (4) and Goodness of Fit Statistics for 6mm Plate

Coefficients (with 95% confidence bounds)	
p_{00}	67.62 (67.61, 67.62)
p_{10}	9.275 (9.267, 9.283)
p_{01}	-48.69 (-48.7, -48.68)
p_{20}	0.8368 (0.8339, 0.8397)
p_{11}	-5.63 (-5.637, -5.624)
p_{02}	25.21 (25.2, 25.22)
p_{30}	-1.236 (-1.24, -1.231)
p_{21}	0.5872 (0.5822, 0.5922)
p_{12}	-0.5615 (-0.5698, -0.5531)
p_{03}	-9.392 (-9.401, -9.383)
p_{31}	0.6049 (0.602, 0.6078)
p_{22}	-0.5281 (-0.5304, -0.5258)
p_{13}	1.644 (1.642, 1.647)
p_{04}	3.398 (3.396, 3.401)
p_{32}	0.1333 (0.13, 0.1367)
p_{23}	0.1289 (0.1262, 0.1316)
p_{14}	-0.5631 (-0.5659, -0.5604)
p_{05}	-0.7749 (-0.7776, -0.7721)
Goodness of fit	
R-square	0.9999
Adjusted R-square	0.9999

In Tables 3.6-3.11, values of R-square and Adjusted R-square being close to unity indicate the high accuracy of the fits.

Chapter 4

Conclusion and Future Scope of Work

❖ ***Conclusion***

A laboratory scale ROT comprising of a furnace, two nozzle banks, cooling bay with roller fitted rails, an air supply circuit, a water supply circuit, an electro-hydraulic actuation system to provide plate movement and a real-time data acquisition system has been fabricated in order to observe the cooling behaviour of MS plates of two different thicknesses under air jet. Effects of other parameters like the air flow rate (Q), initial temperature (T_{in}) of the plate and nozzle bank distance (D) on the same have also been studied.

The thicker plate has taken more time to cool down to room temperature as is quite obvious. The cooling rate (θ) has increased with increase in the air flow rate due to better convection. For some particular parameter settings, the heat transfer coefficient (h) has remained more or less constant up to a certain time, rapidly increasing to the maximum value beyond the same with θ approaching zero. The maximum value of h has been independent of the value of Q. For higher T_{in} , θ has also been higher but more time has been required for the plate to cool down to room temperature. Heat transfer coefficient has reached its maximum value earlier for a lower value of T_{in} but the maximum value of it has not been dependent on T_{in}. Some interesting observations have been encountered in the experimental results regarding the effect of nozzle bank distance (D) on cooling. Up to a certain time, with the average temperature (T_{avg}) of the heated plate being greater than 100^{o}C, θ has increased with D. However, with the T_{avg} value getting reduced further, the relation between θ and D has got reversed. Also, for a particular value of D equal to 85 mm, the plate has taken minimum time to cool down to room temperature. From that particular distance, moving the nozzle bank closer to or away from the plate both has resulted in increase of the cooling time.

Surface plots have also been obtained to find the how T_{avg} is related to Q, T_{in} and D individually. Three separate empirical relations for three of the parameters have been established. Close to unity R-square values of the fitted surfaces indicate that the variation in the experimental dataset have quite satisfactorily been reflected in the mathematical relations drawn. These relations would be quite useful in designing a feedforward control for the system in future.

❖ ***Future Scope of Work***

The results obtained experimentally for air cooling can be substantiated with a numerical analysis of the same problem. Extensive set of experiments should be done on this set up using water and mist for cooling purpose. The effect of the plate velocity should be studied in future by moving the plate with the EHAS. Prediction of a relation involving all the parameters should be attempted in future to obtain an optimized setting of the parameters for a required cooling demand. In this study all the nozzles have been kept open. The effect on cooling can be studied with

changing the number and arrangement of open nozzles. Cooling characteristics of a plate with spray cooling on the bottom surface and natural convection on the top surface can be studied. A closed loop control system combining all the parameters can also be developed in order to get automated setting of the system for some pre-defined cooling curve.

REFERENCES

1. Stewart, I., Massingham, J.D. and Hagers, J.J., Heat Transfer Coefficient Effects on Spray Cooling, Presented at the 1995 AISE Annual Convention and Iron & Steel Exposition, Pittsburgh, Pennsylvania, 27th September, 1995.
2. Longhai, L. and Qiong, Z., Analysis on Influence Factors of the Cooling Efficiency of Moderate Thick Plates in the Quenching with Controlled Cooling, *2nd International Conference on Computer Modeling and Simulation (ICCMS)*, Sanya, Hainan, 390-393, Vol.- 2, 2010.
3. Liu, Z.D., Fraser, D. and Samarasekera, I.V., Experimental Study and Calculation Of Boiling Heat Transfer On Steel Plates During Runout Table Operation, *Canadian Metallurgical Quarterly*, 41, 63 – 74, 2002.
4. Hauksson, A.T., Fraser, D., Prodanovic, V. and Samarasekera, I.V., Experimental study of boiling heat transfer during subcooled water jet impingement on flat steel surface, *Ironmaking and Steelmaking*, 31, 51 – 56, 2004.
5. Sozbir, N., Yigit, C., Issa, R.J., Yao, S.C., Güven, H.R. and Ozcelebi, S., Multiphase spray cooling of steel plates near the Leidenfrost temperature- experimental studies and numerical modeling, Atomization and Sprays, Vol. 20, Issue 5, 387-405, 2010.
6. Oisín F. P., L., Persoons, T., Byrne, G., Darina B., M., Water mist / air jet cooling of a heated plate with variable droplet size**,** *Thermal Issues in Emerging Technologies, ThETA 2*, Cairo, Egypt, 291-296, 2008.
7. Horsky, J. Raudensky, M. and Kotrbacek, P., Experimental Study of Long Product Cooling in Hot Rolling, *Journal of Materials Processing Technology*, 80 – 81, 337 – 340, 1998.
8. Yuan, G., Yu, M., Wang, G.D. and Liu, X.H., Heat transfer of hot strip during ultra fast cooling**,** *Journal of Northeastern University***,** Vol. 27, Issue 4, 406-409, 2006.
9. Wang, H., Yu, W. and Cai, Q., Experimental study of heat transfer coefficient on hot steel plate during water jet impingement cooling**,** *Journal of Materials Processing Technology*, Vol. 212, Issue 9, 1825-1831, 2012.
10. Hosain, M.L., Fdhila, R.B. and Daneryd, A., Multi-jet impingement cooling of a hot flat steel plate, *Energy Procedia*, Vol. 61, 1835-1839, 2014.
11. Wang, H.M., Cai, Q.W., Yu, W. and Su, L., Effect of water flow rate on the heat transfer coefficient of a hot steel plate during laminar flow cooling, *Journal of University of Science and Technology Beijing*, Volume 34, Issue 12, Pages 1421-1425, 2012.
12. Lee, P., Choi, H. and Lee, S., The effect of nozzle height on cooling heat transfer from a hot steel plate by an impinging liquid jet, *ISIJ International*, Vol. 44, Issue 4, 704-709, 2004.
13. Wang, B., Lin, D., Xie, Q., Wang, Z. and Wang, G., *Applied Thermal Engineering*, Vol. 100, Pages 902-910, 2016.
14. Mukhopadhyay, A. and Sikdar, S., Implementation of an on-line run-out table model in a hot strip mill, *Journal of Materials Processing Technology*, 169, 164 – 172, 2005.
15. Barman, S., Barman, N., Mukhopadhyay, A. and Sen, S., Thermal Behavior of a Hot Moving Steel Strip Under Multi-Cooling Jets, *Heat Transfer Engineering*, Vol. 35, Issue 14-15, 1363-1369, 2014.
16. Samanta, S., Mukherjee, S., Dhar, M., Barman, S., Barman, N., Mukhopadhyay, A. and Sen, S., Heatline based thermal behaviour during cooling of a hot moving steel plate using single jet, *Applied Mechanics and Materials*, Vol. 592-594, 1622-1626, 2014.
17. Mandal, P., Actuation System Design (English), *LAP Lambert Academic Publishing*, ISBN-10-3845443650, 2011.